ANL/ET/CP-102247

Structural and Electrical Properties of Biaxially Textured $YBa_2Cu_3O_{7-x}$ Thin Films on Buffered Ni-Based Alloy Substrates*

M. Li, B. Ma, Y. A. Jee, B. L. Fisher, and U. Balachandran
Energy Technology Division, Argonne National Laboratory
Argonne, Illinois 60439

November 2000

Manuscript submitted to the Proceedings of the Materials Research Society Fall Meeting, Boston, Nov. 27-Dec. 1, 2000.

*Work supported by U.S. Department of Energy (DOE), Energy Efficiency and Renewable Energy, as part of a DOE program to develop electric power technology, under Contract W-31-109-Eng-38.

DISCLAIMER

Structural and Electrical Properties of Biaxially Textured $YBa_2Cu_3O_{7-x}$ Thin Films on Buffered Ni-based Alloy Substrates

M. Li, B. Ma, Y. A. Jee, B. L. Fisher, and U. Balachandran

Argonne National Laboratory, Argonne, IL 60439

Abstract

Oxide high-T_c superconducting wires and tapes with high critical current density (J_c) are essential in future electrical power applications. Recently, $YBa_2Cu_3O_{7-x}$ (YBCO) thin films grown on Ni-based alloy tapes have attracted intense interest because of their promise for these applications. In order to achieve high J_c, buffer layers are necessary for fabricating biaxially aligned YBCO thin films. In our studies, yttria-stabilized zirconia (YSZ) layers were deposited on Ni-based alloy substrate by ion-beam assisted deposition, and CeO_2 buffer layers were subsequently deposited on the YSZ layer by pulsed laser deposition (PLD) or electron beam evaporation. In addition, MgO layers were deposited on Ni-based alloy substrates by inclined substrate deposition. Finally, biaxially textured YBCO thin films were deposited on these buffered metallic substrates by PLD under optimized conditions. The orientation and in-plane textures of YBCO and the buffer layers were characterized by X-ray diffraction $\theta/2\theta$ scan, ϕ-scan, and pole figure analysis. The superconductive transition features were examined by measuring inductive T_c and transport J_c .

1. Introduction

Oxide superconducting films with high transition temperature (T_c) and high critical current density (J_c) on polycrystalline metal tape substrates are needed for power applications [1-5]. It is known that the J_c of polycrystalline high-T_c superconducting films is limited by the weak-link behavior of grain boundaries in the films. To reduce these influences, it is essential to grow biaxially aligned high-T_c superconducting films.

Unlike the Bi-Sr-Ca-Cu-O system, $YBa_2Cu_3O_{7-x}$ (YBCO) thin films have the advantages of strong pinning properties without the artificial introduction of pinning centers. High-current electric power application can be achieved if high-J_c YBCO films could be grown on biaxially textured metal substrates.

The Ni-based alloy, Hastelloy C (HC), is desirable for use as in substrate because of its resistance to oxidation at high temperature, its closely matched thermal expansion coefficient with YBCO, and its availability in long lengths and thin tapes.

Several techniques have been employed to fabricate biaxially textured templates on the Ni-based alloy metal substrates such as ion-beam-assisted deposition (IBAD) and inclined substrate deposition (ISD). The IBAD technique is effective in fabricating biaxially textured templates on polycrystalline substrates. Yttria-stabilized zirconia (YSZ) with biaxial texture can be obtained on the Ni-based substrates by this technique [2,4]. The YSZ layer will serve as a template for growth of textured YBCO film and as a diffusion barrier between the YBCO film and the substrate. ISD is a very promising method because of its very high deposition rate of up to 500 nm/min, thus minimizing the time for the coating of long tapes [5]. YBCO can be subsequently deposited on these buffered substrates by pulsed laser deposition (PLD). In this paper, we report the successful growth by PLD and the properties of biaxially aligned YBCO films on these biaxially buffered Ni-based metal substrates.

2. Experiments

YBCO films were deposited by the PLD method. An excimer laser (Lamda Physik, Compex 201) with wavelength of 248 nm and pulse width of 25 ns was used for the deposition. A pulse energy of 160 mJ, pulse repeat rate of 8 Hz, and oxygen pressure of 250 mtorr were employed. For deposition of CeO_2 layer, 1 Hz and 300 mtorr of oxygen pressure were used. The substrates, which were mounted on a heatable sample stage with silver paste, were heated to the desired deposition substrate temperature (T_s). Distance between the target and the substrates was 7.5 cm.

Hastelloy C was polished and used as the substrate. Both the biaxially textured YSZ layer deposited by IBAD and the MgO layer deposited by ISD were employed as buffer layers for YBCO films. Electron beam evaporation and ion beam assistance with a incident angle of 55° with respect to the substrate normal were adopted in our IBAD system [6]. Typical thickness of the YSZ buffer layer was 1 μm. The MgO layer was deposited by electron beam evaporation at room temperature with a substrate inclined angle of 50° with respect to the evaporating beam and at a growth rate of 5 nm/s. Typical thickness of the ISD MgO layer was 2 μm.

The structure of these films was examined by X-ray diffraction. The out-of-plane texture of the films were investigated by θ/2θ scan and Omega-scan, while the in-plane texture was examined by a pole figure and ϕ-scan measurement. Film texture and cation disorder were characterized by Raman spectra analysis. The T_c was measured by the inductive method. The J_c values of some of these samples were obtained by the standard four-point method with a voltage criteria of 1 μV/cm.

3. Results and Discussions

YBCO films grown on MgO(ISD)/HC substrates

YBCO films were deposited on MgO(ISD)/HC substrates by PLD under optimized condition. X-ray pole figure measurement shows clear biaxial texture for both the YBCO film and the MgO (ISD) layer (Figure 1). The asymmetrical distribution of the pole peaks indicates the tilt features of the (00l) crystalline plane of the YBCO film and the MgO layer. The tilt angles of the MgO layer and of the YBCO film derived from the pattern have about the same value of 31°. The strong and narrow pole peaks suggest that both the film and the buffer layer have good in-plane and out-of-plane texture, revealing epitaxial growth of a usual cube on cube orientation of YBCO[001] // MgO[001] and YBCO[100]//MgO[100] (or [010]). To characterize in-plane texture, X-ray ϕ-scans of the sample were performed. Figure 2 shows X-ray ϕ-scan patterns of the sample from (a) YBCO(103) and (b) MgO(220). The full-width-at-half-maximum (FWHM) were 12.2° for YBCO(103) and 12.8° for MgO(220), respectively.

YBCO films grown on YSZ(IBAD)/HC substrates

YBCO films were fabricated by PLD on biaxially buffered Hastelloy C substrates. X-ray diffraction $\theta/2\theta$ scan patterns of the YBCO film grown on biaxially textured Hastelloy C substrates are shown in Figure 3. Strong and sharp (00l) peaks in the patterns indicate a highly-c-axis orientation in these films. For the YBCO film grown directly on YSZ-buffered HC, a-axis orientation peaks of (100) and (200) can be seen from the XRD pattern. A-axis orientation is believed not to contribute to the superconducting properties of the YBCO film. In order to improve the lattice match between the YBCO film and the YSZ buffer layer, a CeO_2 buffer layer was deposited on YSZ/HC by PLD [7]. No a-axis orientation peaks can be found and a fully c-axis orientation of the film was formed, as shown in Figure 3(b).

The in-plane textures of these YBCO films were characterized by X-ray ϕ-scan analysis (Figure 4), which indicated that the YBCO, CeO_2, and YSZ buffer layer have good in-plane cube-to-cube relationships, with YBCO[100]//CeO_2[100]//YSZ[100]. The FWHM of the ϕ-scan diffraction peaks for the selected plane of each layer gives the divergence of the in-plane orientation, which are 14°, 17.5°, and 18° for the YBCO(103), CeO2(111), and YSZ(111), respectively. Films with lower FWHM values could be expected to have higher critical current [8].

Raman spectra have also been used to evaluate the quality of the as-grown YBCO films. Figure 5 gives the Raman spectra of the YBCO films. Compared with the film grown on YSZ-buffered substrate, improvement can be clearly seen in the Raman spectrum of the YBCO film with a double buffer layer of CeO_2/YSZ. The only strong peaks in the 340 cm^{-1} Raman shift indicates the formation of a good epitaxial film, while in the Raman spectrum of the YBCO film with only a YSZ buffer layer, the corresponding $\approx$340 cm^{-1} peak is relatively weak. The strong peak in about $\approx$500 cm^{-1} of Raman shift corresponds to texture puckering of the YBCO film.

The electrical properties of YBCO films are characterized by measuring the superconducting transition temperature (T_c) and the critical current density J_c. Typical T_c values are given in Figure 6. T_c values of 88-90 K with narrow transition width are usually observed in films with a double buffer layer of CeO_2/YSZ. The highest J_c of 8.4×10^5 A/cm^2 was obtained in a 1-µm-thick YBCO film on CeO_2/YSZ-buffered Ni-based alloy substrate.

4. Conclusions

(1) Biaxially textured YBCO film was successfully grown by pulsed laser deposition on inclined substrate deposition MgO-buffered polycrystalline metal substrates. The c-

axis of the YBCO films tilt 31° with respect to the normal of the substrate. The FWHM values of the ϕ-scan of YBCO(103) and MgO(220) were 12° and 12.8°, respectively.

(2) High-quality c-axis oriented biaxially textured YBCO films were deposited on yttria-stabilized zirconia (YSZ) buffered metal substrates. X-ray pole-figure and ϕ-scan indicate that these films have good in-plane texture and that the FWHM values of the samples are 14° for YBCO film and 18° for the YSZ layer. X-ray diffraction, Raman spectra, and electrical property measurement indicated that by introducing an additional CeO_2 buffer layer, the quality of the YBCO films can be effectively improved with respect to microstructure, cation disorder, and superconducting transition width of the film..

(3) Compared with the results obtained on the YBCO films grown on ISD MgO-buffered substrate and IBAD YSZ-buffered substrate, it can be seen that the microstructure and the orientation of the buffer layer play important roles in the growth of YBCO film. The tilted c-axis orientation of the YBCO films have a negative influence on the structure and electrical properties of the YBCO films.

Acknowledgments

The Authors thank Dr. Victor Maroni for Raman spectroscopy measurements. This work is supported by the U.S. Department of Energy (DOE), Energy Efficiency and Renewable Energy, as part of a DOE program to develop electric power technology, under Contract W-31-109-Eng-38.

References

1. Y. Iijima, N. Tanabe, O. Kohno, and Y. Ikeno, Appl. Phys. Lett., 60(6), 769(1992)

2. D. P. Norton, A. Goyal, J. D. Budai, D. K. Christen, D. M. Kroeger, E. D. Specht, Q. He, B. Saffian, M. Paranthaman, C. E. Klabunde, D. F. Lee, B. C. Sales, and F. A. List, Science, 274, 755(1996)

3. X. D. Wu, S. R. Foltyn, P. N. Arendt, W. R. Blumenthal, I. H. Campbell, J. D. Cotton, J. Y. Coulter, W. L. Hults, M. P. Maley, H. F. Safar, and J. L. Smith, Appl. Phys. Lett., 67(16), 2397(1995)

4. Y. Iijima, M. Hosaka, N. Tanabe, N. Sadakata, T. Saitoh, O. Kohno, and K. Takeda, J. Mater. Res., 12(11), 2913 (1997)

5. M. Bauer, R. Semerad, and H. Kinder, IEEE Transactions on Applied Superconductivity, 9(2), 1502(1999)

6. M. P. Chudzik, R. Erck, M. T. Lanagan, and C. R. Kannewurf, IEEE Transactions on Applied Superconductivity, 9(2), 1490 (1999)

7. X. D. Wu, R. C. Dye, R. E. Muenchausen, S. R. Foltyn, M. Maley, A. D. Rollett, A. R. Garcia, and N. S. Nogar, Appl. Phys. Lett., 58(19), 2165 (1991)

8. A. Knierim, R. Auer, J. Geerk, G. Linker, O. Meyer, H. Reiner, and R. Schneider, Appl. Phys. Lett., 70(5), 66(1997)

Figure Captions

Figure 1. Pole figure patterns of YBCO(103) on MgO-buffered HC substrate. Asymmetrical distribution of pole peaks indicates tilt features of (00l) crystalline plane of YBCO film. Tilt angle deduced from the pattern is 31° for YBCO film.

Figure 2. ϕ-scan patterns of (a) MgO(220) and (b) YBCO(103) on MgO-buffered HC substrate. FWHM values of YBCO(103) and MgO(220) are 12.2° and 12.8°, respectively.

Figure 3. X-ray θ-2θ diffraction pattern of (a) YBCO/YSZ/HC and (b) YBCO/CeO_2/YSZ/HC samples. YBCO (l00) peaks are masked by growth of CeO_2 buffer layer.

Fugure 4. ϕ-scan of YBCO/CeO_2/YSZ/HC films. FWHM =14° for YBCO(103) and 18° for YSZ(111).

Figure 5. Raman spectra of YBCO films grown on (a) YSZ buffered HC substrates and (b) with additional CeO_2 buffer layer.

Figure 6. Critical transition temperature, T_c, of YBCO films grown on (a) YSZ buffered and (b) CeO_2/YSZ buffered HC substrates, respectively.

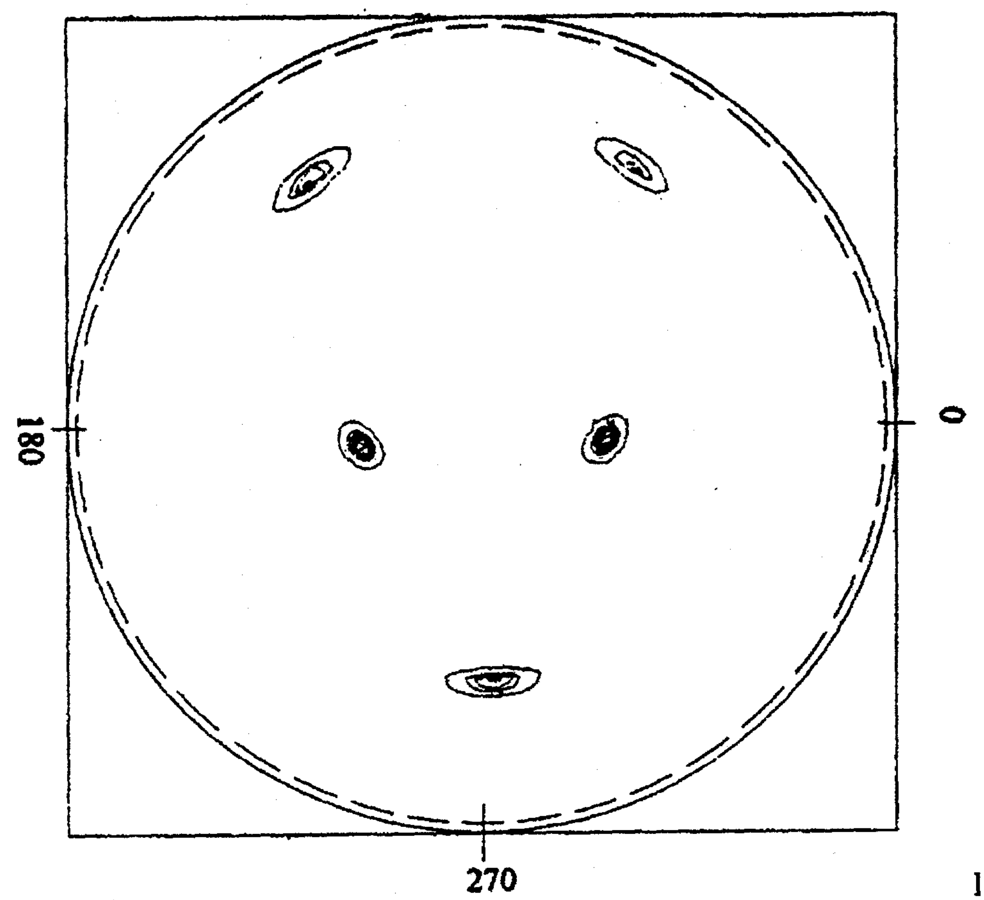

Figure 1

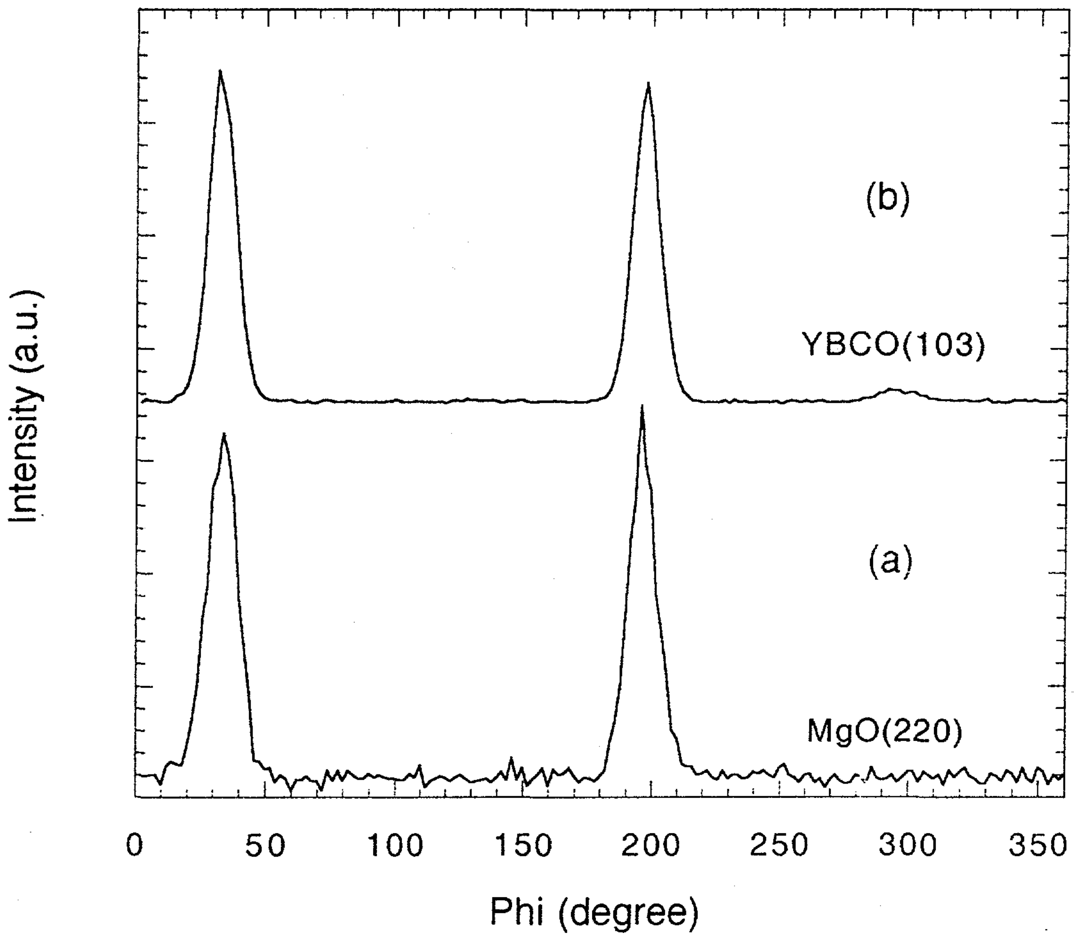
Intensity (a.u.)
(b)
YBCO(103)
(a)
MgO(220)
0
50
100
150
200
250
300
350
Phi (degree)

Figure 2

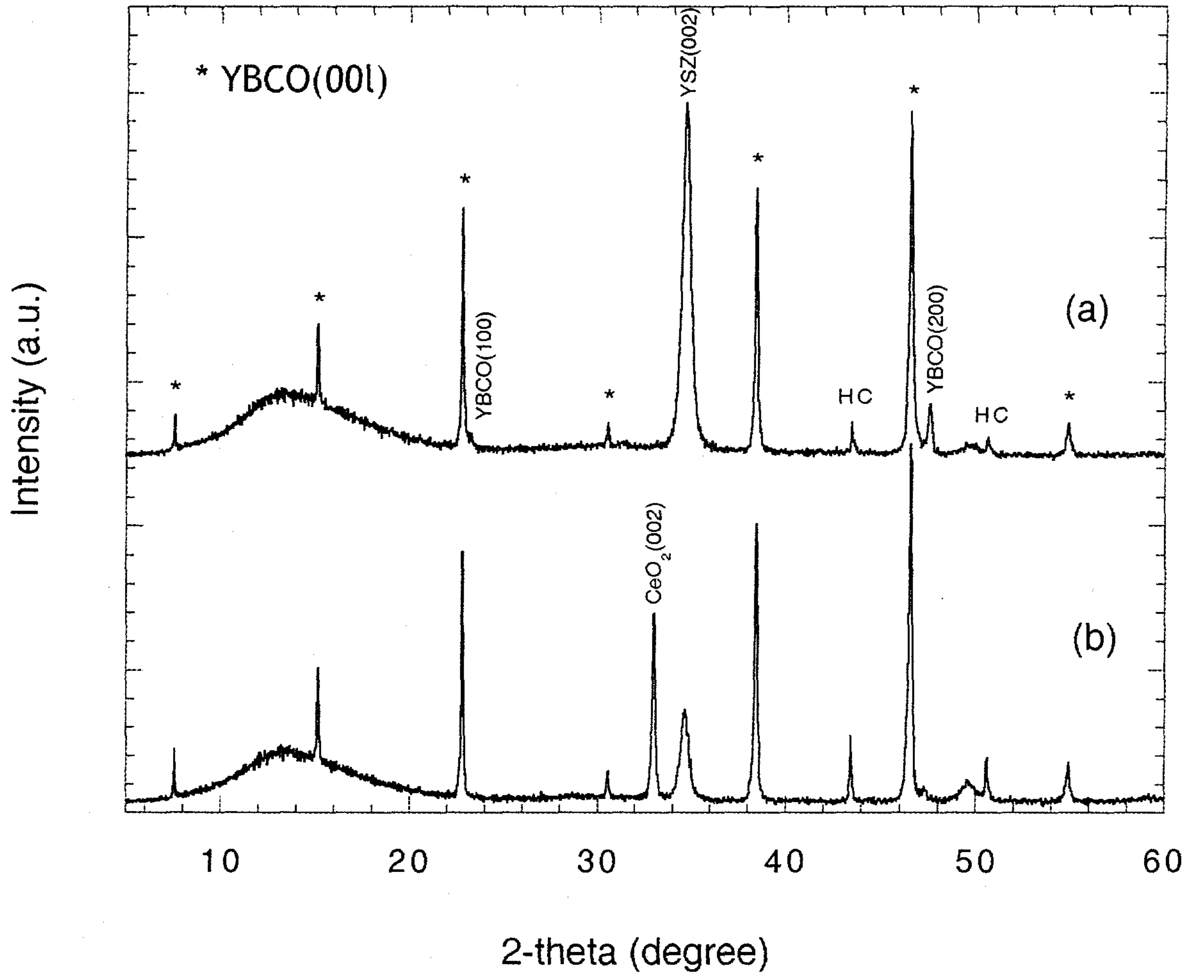
* YBCO(00l)
YSZ(002)
YBCO(100)
YBCO(200)
HC
HC
CeO2(002)
(a)
(b)
Intensity (a.u.)
10
20
30
40
50
60
2-theta (degree)

Figure 3

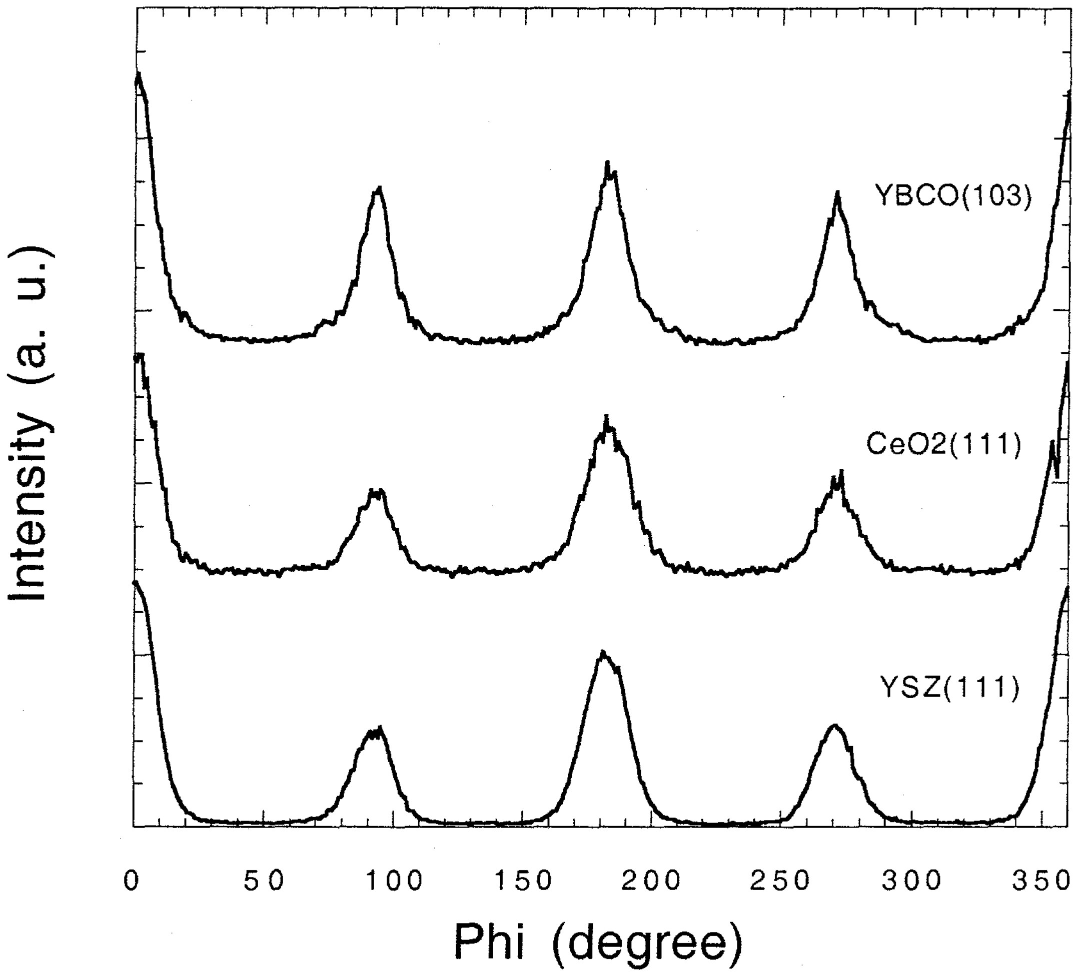
YBCO(103)
CeO2(111)
YSZ(111)
Intensity (a. u.)
0
50
100
150
200
250
300
350
Phi (degree)

Figure 4

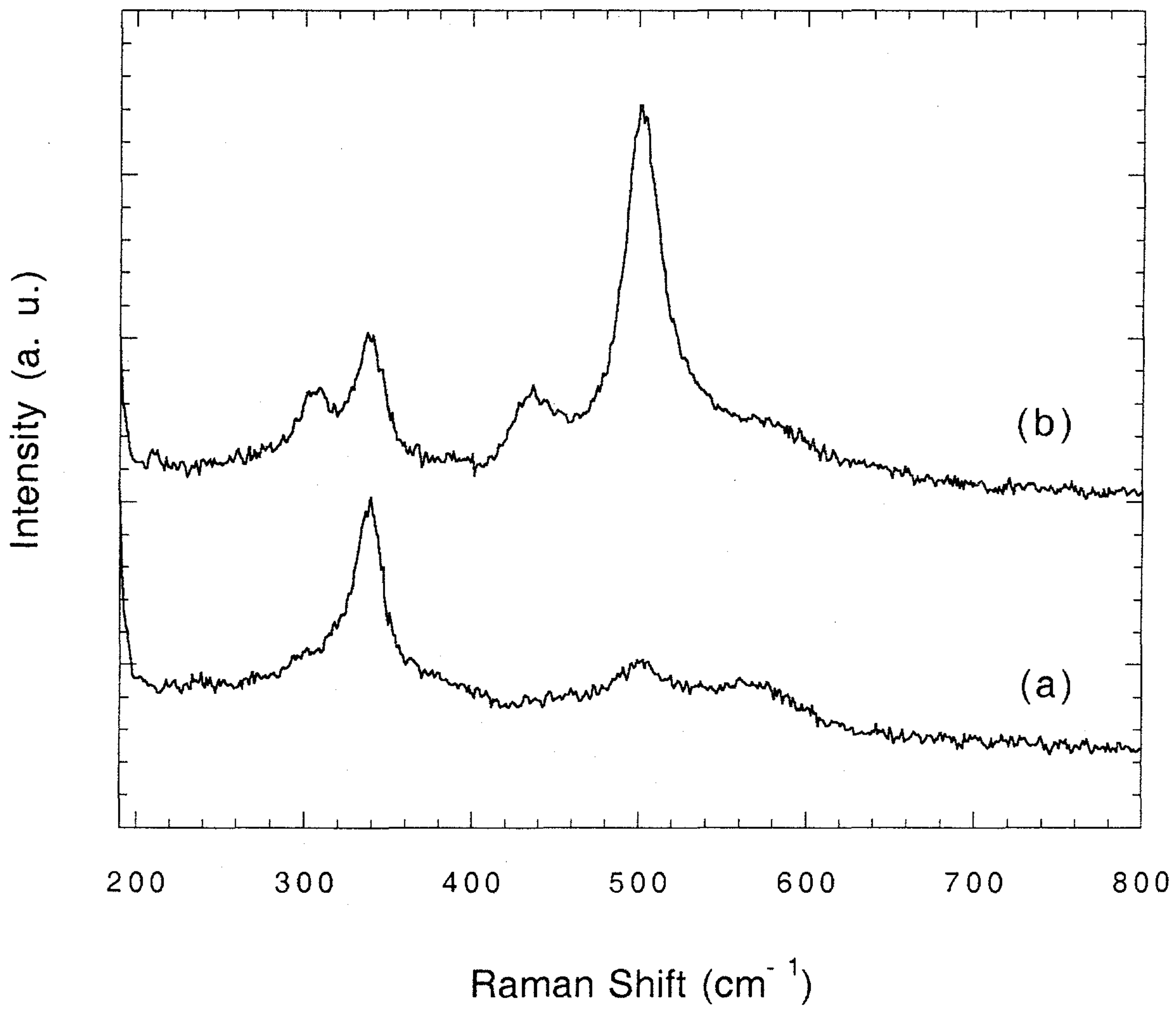

Figure 5

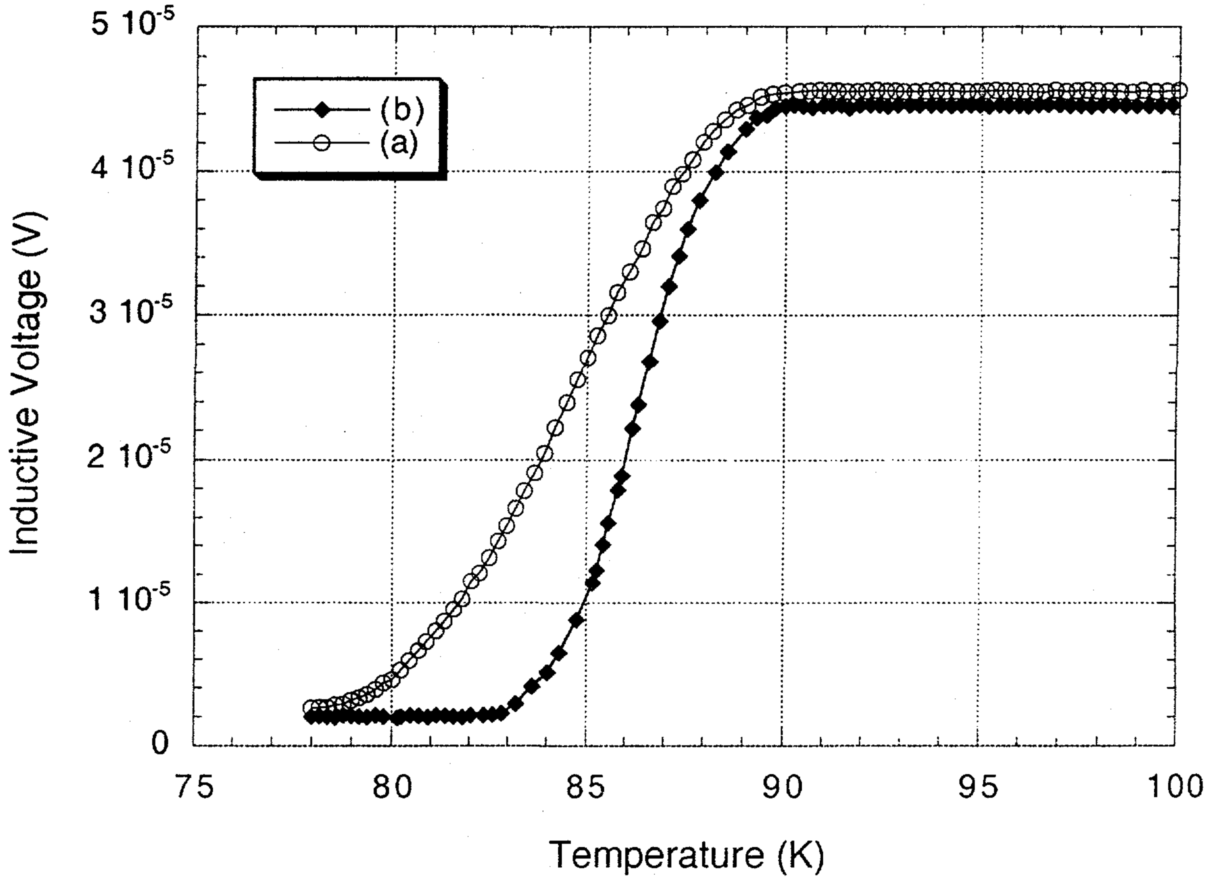

(b)
(a)
5 10-5
4 10-5
3 10-5
2 10-5
1 10-5
0
Inductive Voltage (V)
75
80
85
90
95
100
Temperature (K)

Figure 6